


Structural, morphological, and magnetic properties of copper zinc cobalt ferrites systems nanocomposites

Arthur Charles Prabakar¹, Govindarasu Killivalavan¹, Dhananjayan Sivakumar², K. Chandra Babu Naidu³, Balaraman Sathyaseelan^{4,*} , Krishnamoorthy Senthilnathan⁵, Iruson Baskaran⁶, Elayaperumal Manikandan⁷, B. Ramakrishna Rao⁸, M.S.S.R.K.N. Sarma³, A. Ratnamala⁸

¹ Research and Development Center, Bharathiar University, Coimbatore-641046, India

² Department of Physics, Sree Krishna College of Engineering, Unai, Anaicut-632101, Tamilnadu, India

³ Department of Physics, GITAM Deemed to be University, Bangalore-562163, Karnataka, India

⁴ Department of Physics, University College of Engineering Arni, Anna University Chennai, Arni 632326, Tamil Nadu, India

⁵ Photonics Division, School of Advanced Sciences, VIT University, Vellore, 632014, Tamil Nadu, India

⁶ Department of Physics Arignar Anna Government Arts College, Cheyyar 604407, Tamil Nadu, India

⁷ Department of Physics, Thiruvalluvar University College of Arts and Science, Thennangur Village, Vandavasi Taluk, Tiruvannamalai District 604408, India

⁸ Department of Chemistry, GITAM Deemed to be University, Bangalore-562163, Karnataka, India

*corresponding author e-mail address: bsseelan03@gmail.com | Scopus ID [35734996700](https://orcid.org/0000-0001-9148-7700)

ABSTRACT

In this study, by the method of co-precipitation with PEG as surfactant as agent nanocomposite of the Copper Zinc Cobalt ferrites systems (CuZnCoFO NCs) are prepared. The X-ray diffraction (XRD), transmission electron microscopy, and field emission scanning electron microscopy of the samples are carried out. To analyse the magnetic measurements the samples are subjected to the vibrating sample magnetometer (VSM). The results of the paramagnetic properties formed out of chemical precipitation method are effective at room temperature. These ferrite system nanoparticles with magnetic fields could have effective application. The photocatalyst activity when annealed at 600°C at 2h NPs is also evaluated by Methylene Blue degradation when exposed to ultraviolet light irradiation.

Keywords: Ferrite, nanocomposite, XRD, TEM, magnetic properties.

1. INTRODUCTION

Spinel ferrite particles in nano dimension exhibit appealing and extraordinary properties compared to their bulk samples [1]. The reduction of organic dopants through the Photocatalytic degradation on the surface of semiconductor is the most promising and reliable technique. In comparison with iron oxide many large catalytic phenomenon. The obtained ferrite system was also ferrite nanoparticles perform peroxidase-like activity towards Mg, Co, and Cu ferrite system which yield excellent catalysts and possess excellent potential with chemical compositions that leads doping of non-metal [6-8], transition metal [9, 10] and noble metal [11-13].

Also it is possible to develop unique properties to the nanocomposites by different ferrite oxides with spinel structures [14]. Spinel structures have the general formula AB₂O₄, with A as a divalent cation (Co²⁺, Zn²⁺) and B as a trivalent cation (Fe³⁺, Cr³⁺) [15-16]. Ferrites are spinel structure in which B sites are occupied with Fe³⁺ cations to form ferromagnetic compound.

The Spinel ferrites (MFe₂O₄) perform extremely well during advanced oxidation processes (AOPs), due to their narrow energy band gap (2 eV) [19], and is also used to alter the properties of the catalyst by using a metal with strong magnetic properties.

2. MATERIALS AND METHODS

2.1. Material Synthesis.

The sample is meticulously prepared. The characteristic behaviour of the nanocomposites has great impact on the preparation process. [29]. Ferric nitrate (98%), cupric nitrate (99.5%), zinc nitrate (96%), cobalt nitrate (99%), salts are taken

In this way, the catalyst is easily recovered during wastewater management [20]. Moreover, ferrites in the spinel structure, formed by multiple metals, decide the permanent properties of the catalyst [21].

He *et al.* reported the photo degradation of Methylene blue dye using catalyst Zn_{1-x}Co_xFe₂O₄ [22], due to its strong magnetic field influence the Zn and Co-ferrite phase and narrow energy band gap. The nanoparticles have a wide applications that are prepared by methods like, co-precipitation [23], ultrasound-assisted emulsification [24], hydrothermal [25], sol-gel [26] and microwave solid - state techniques [27]. Among the various type of spinel ferrite Nanoparticles, zinc ferrite nanoparticles exhibit endearing magnetic properties [28] and its performance mostly depends on their stoichiometric ratio and structures (micro), which vary by the methods of synthesizing.

In the present work, the preparation, depiction, evaluation and photo catalytic performances of the new removal catalyst Copper Zinc Cobalt ferrites systems (CZCFO NCs) for the removal of Methylene blue dye using solar irradiation is studied. To achieve the desired properties and to ensure strong magnetic properties of ferrites systems Copper Zinc Cobalt's unification was made.

and the required sample is arrived by modifying the co-precipitation method.

Two solutions of molarity 0.1 are mixed well using a stirrer maintained at a temperature of 80°C until the mixture turns into dark brown. Polyethylene glycol oxide powder of 0.2 g is added gently

to the product in order basicity; excess of NH_3 is later added. The extracted paste is sintered in an oven at 150°C for 24 h. Then the prepared sample is annealed at temperature 500 and 600°C under thermal control which is finally well ground.

2.2. Instrumentation and Apparatus.

The structure and phase purity of Copper Zinc Cobalt ferrites systems (CZCFO NCs) Nano composite was observed by X-ray powder Diffractometer. The morphology and selected area electron diffraction pattern are analyzed by the transmission electron microscopy. In addition Copper Zinc Cobalt ferrites systems

3. RESULTS

3.1. Structure and crystalline nature of the obtained copper zinc cobalt ferrites systems (CZCFO NCs) nanocomposite.

Figure 1 exhibits that the XRD pattern of the nanocomposites at room temperature possesses a cubic spinel structure [29]. In the XRD pattern the intensity of (311) reflections is strong, indicating the preferred orientation along the (311) direction. The other peaks (111), (200), (220), (400), (411), (422) and (511) are also observed.

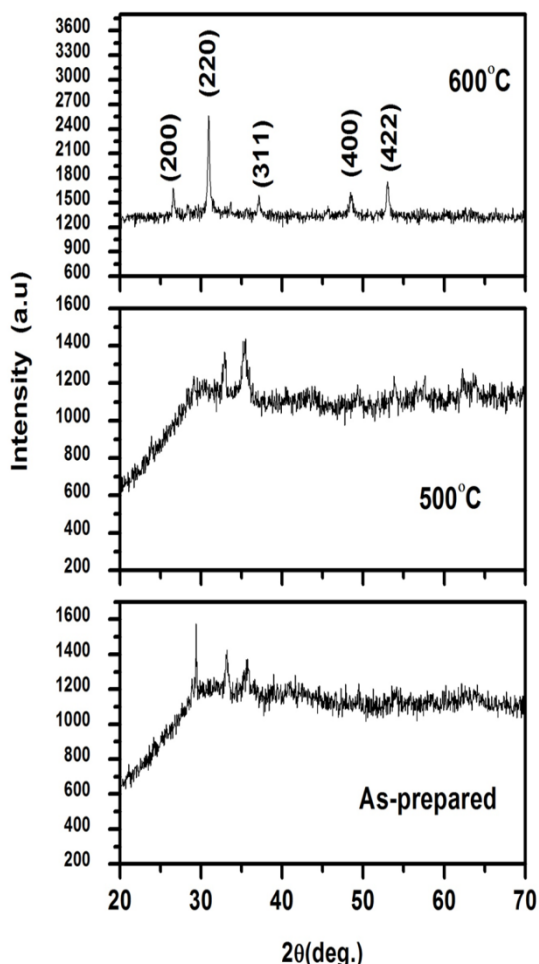


Figure 1. Powder XRD of copper zinc cobalt ferrites systems (CZCFO NCs) nanocomposites.

The X-ray diffraction also confirms the fcc spinel structure with a single phase for all the samples, and the broad lines acknowledge the nano size of the samples. The estimated final contents agree with the initial ratio and the broad lines acknowledge the nano size of the samples. From the (3 1 1) plane using Debye-Scherrer formula, the particles size is measured.

(CZCFO NCs) nanocomposites photo catalytic activity was examined through MB in UV light irradiation by photoreactor (HML MP88.).

Fourier transform infrared spectra (FTIR) of Copper Zinc Cobalt Ferrites Systems (CZCFO NCs) nanocomposites were developed in the range of $2000 - 400\text{ cm}^{-1}$ wavenumber. For improved physical and magnetic character, the sample is annealed at 600°C sample and analysed through Vibrating Sample Magnetometer.

3.2. Microstructural analysis through scanning electron microscopy (SEM) and fundamental attributes of the copper zinc cobalt ferrites systems (CZCFO NCs) Nano composite.

Figures 2 show the SEM images of Copper Zinc Cobalt ferrites systems (CZCFO NCs) Nano composites. The SEM images emphasize the collection of particles with some residue. Porosity is formed at the junctions. It could be observed from the graph that the grains of the Zn-Cu-Co are rigid and paves for oxygen adsorption on its surface.

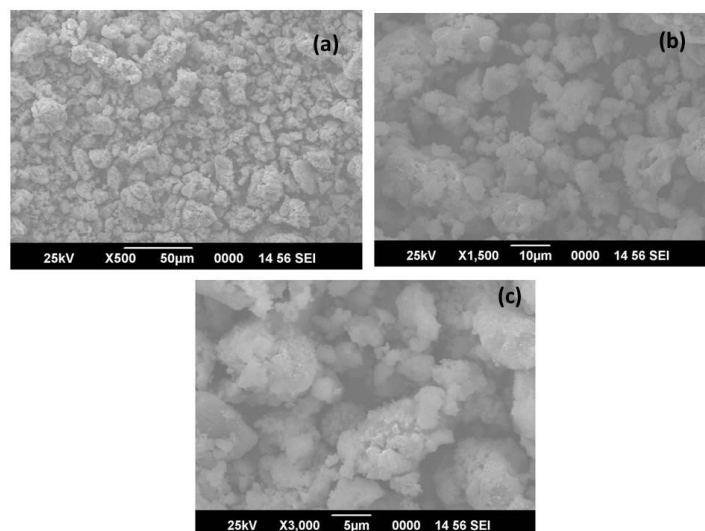


Figure 2. SEM images of copper zinc cobalt ferrites systems (CZCFO NCs) nanocomposites at (a) as-prepared (b) annealed at 500°C (c) annealed at 600°C .

During TEM imaging the EDX spectra were recorded at multiple positions of the sample to confirm the chemical constituents of the (CZCFO NCs) nanocomposites (Fig 3). The chemical attributes match with the experimental data. The stoichiometric proportions of Cu, Co, Zn, Fe, and O elements are identical with the ferrite crystallites in the sample. The presence of Na arises from the grid, supports carbon film. The EDX for the heated sample also exhibits synonyms composition.

All these studies acknowledge that the synthesized material obtained by co-precipitation protocol were particles of (CZCFO NCs) nanocomposites.

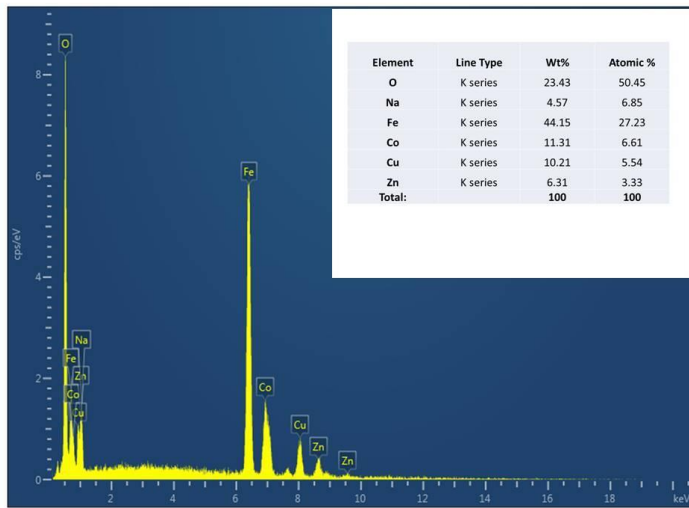


Figure 3. EDX spectra of Copper Zinc Cobalt Ferrites Systems (CZCFO NCs) Nanocomposites at (a) annealed at 600°C.

The chemical constituents of the composites were also viewed by an energy dispersive spectroscopy (EDX). The Na, O, Zn, Cu, Co and Fe peaks in EDX spectra confirm the presence of sodium, oxygen, Zinc, copper, cobalt and ferrite system.

3.3. Morphological study of the copper zinc cobalt ferrites systems (CZCFO NCs) nanocomposite by transmission electron microscopy and selected area electron diffraction (SAED).

The morphology and shape of the nanocomposite were examined. When examined using high-resolving transmission electron microscopy due to nano size, single-field the particles are permanently magnetized and experience a magnetic moment proportional to their volume. The particles with size less than 15nm are grouped. After crystallinity, the sample with cubic spinel crystal structure confirms the electron diffraction (ED) profile. (Fig.4).

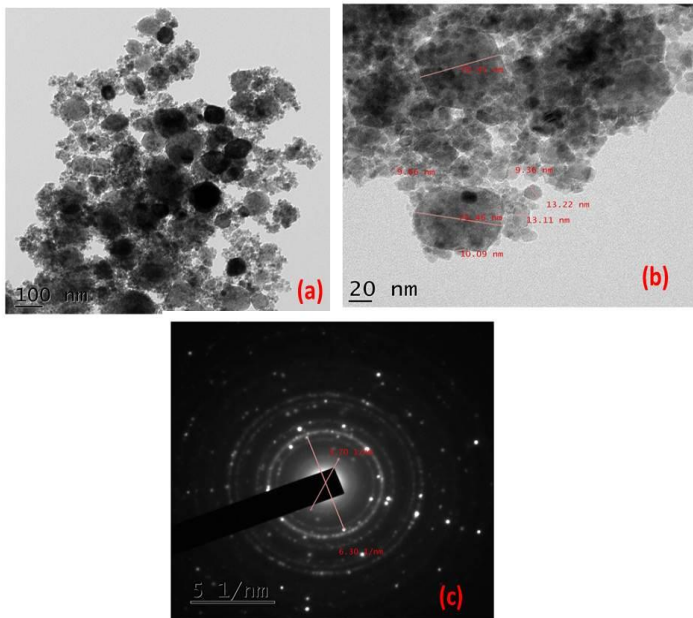


Figure 4. TEM images of copper zinc cobalt ferrites systems (CZCFO NCs) Nano composites (a) annealed at 600°C (b) SAED.

The selected area electron diffraction (SAED) picture of the sample estimated the d-spacing as 2.541 Å indicates that the initial concentric ring corresponds to (311) plane of Copper Zinc Cobalt ferrites systems (CZCFO NCs) nanocomposites. (JCPDS powder diffraction) Similarly, other fringes were assigned as (422) (511)

and (440) planes. The sample once again confirms the ED profile analysis.

3.4. FTIR study of copper zinc cobalt ferrites systems (CZCFO NCs) nanocomposite.

The extensive metal-oxygen bands are shown by the FTIR spectra (Fig-5). The vibration of metal in tetrahedral site has wave number in the range 400 cm-1 to 500 cm-1. The bands in the range of 500 cm-1 to 600 cm-1 are identified as octahedral stretching. The Mtetra ↔ O bands are observed at 478 cm-1,509 cm-1, 586 cm-1 and 393 cm-1. The absorption bands found at 3404cm-1 indicates the presence of adsorbed water on the surface of the ferrite nano particles.

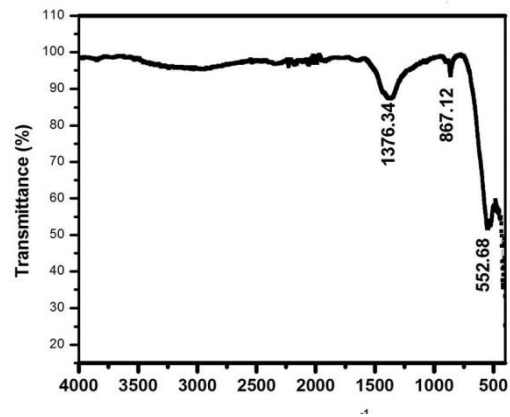


Figure 5. FTIR spectra of copper zinc cobalt ferrites systems (CZCFO NCs) nanocomposites.

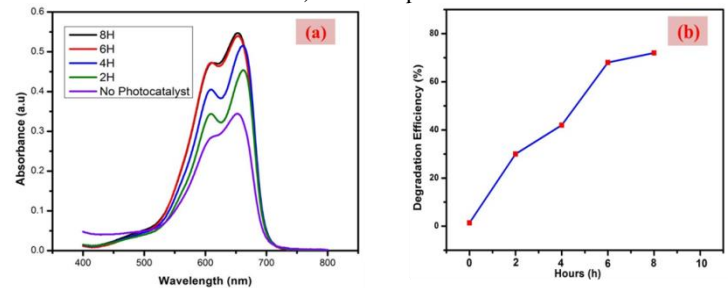


Figure 6. Copper zinc cobalt ferrites systems (CZCFO NCs) nanocomposites annealed at 600°C under UV-light irradiation (a) Absorption of MB solution during the photo degradation (b) Photo degradation percentage.

3.5. Photocatalytic analysis of copper zinc cobalt ferrites systems (CZCFO NCs) Nano composite

The absorbance versus wavelength graph and degradation efficiency with respect to time of (CZCFO NCs) nano composites during photocatalytic degradation of MB dye under UV light irradiation is shown in Fig.6. Thirty (30) mg of Copper Zinc Cobalt ferrites systems (CZCFO NCs) nano composites catalyst was dispensed in 10 ppm of MB dye and photo degradation was evaluated with 10 mg/L. Using photochemical reactor, the solution was irradiated by UV radiation and from the resultant, 2 mL were withdrawn at every 20 mins intervals in 300 mins duration.

The photo degradation of the collected aqueous solution was measured using a UV - Visible spectrometer [31]. Generally light absorbing catalyst generate electron-hole pair which produce H and O₂⁻ ions at the surface of the catalyst. The degradation efficiency of MB under UV light irradiation is determined to be 72% with enhanced time interval.

3.6. Magnetic parameters of copper zinc cobalt ferrites systems (CZCFO NCs) nanocomposite at room temperature.

The hysteric loop obtained in fig.7. reveals the magnitude of the magnetic features such as magnetic saturation (M_s), coercivity (H_c) and remanence (M_r) for the prepared nanocomposites. The results exhibit that the samples having smaller grains are estimated to have low coercivity, and vice versa. The size may be the general reason for the reduction in the coercivity of the ferrites system [30, 31]. It can be noticed the value of coercivity (H_c) of the ferrite samples, thereby indicates that these materials are soft magnetic materials.

The reason for the reduction in saturation magnetization is due to the movement of ferric ions from B to A region [32]. In our study ' M_s ' magnetic saturation (36.818 emu/g) and ' H_c ' coercivity values (99.738 G) found to be high and the value of H_c seems to be low. Hence the synthesized Copper Zinc Cobalt Ferrites Systems (CZCFO NCs) Nanocomposites are apt for low core losses on transformers.

The value of Squareness of Copper Zinc Cobalt ferrites systems (CZCFO NCs) is estimated to be 0.1. If the ratio M_r/M_s is

4. CONCLUSIONS

The Spinel Copper Zinc Cobalt ferrites systems (CZCFO NCs) Nanocomposites were carefully prepared by chemical precipitation method with necessary precautions. The cubic inverse spinel structures of the prepared sample were confirmed by X-ray diffraction. The crystalline nature of the nanocomposites is

5. REFERENCES

1. Burda, C.; Chen, X.; Narayanan, R.; El-Sayed, M.A. Chemistry and Properties of Nanocrystals of Different Shapes. *Chemical Reviews* **2005**, *105*, 1025-1102, <http://dx.doi.org/10.1021/cr030063a>.
2. Anicete-Santos, M.; Orhan, E.; De Maurera, M.; Simoes, L.G.P.; Souza, A.G.; Pizani, P.S.; Leite, E.R.; Varela, J.A.; Andrés, J.; Beltrán, A. Contribution of structural order-disorder to the green photoluminescence of $Pb\ W\ O_4$. *Physical Review B* **2007**, *75*, <https://doi.org/10.1103/PhysRevB.75.165105>.
3. Ryu, J.H.; Yoon, J.-W.; Shim, K.B. Blue luminescence of nanocrystalline $PbWO_4$ phosphor synthesized via a citrate complex route assisted by microwave irradiation. *Solid state communications* **2005**, *133*, 657-661, <https://doi.org/10.1016/j.ssc.2004.12.046>
4. Ryu, J.H.; Yoon, J.-W.; Lim, C.S.; Oh, W.-C.; Shim, K.B. Microwave-assisted synthesis of $CaMoO_4$ nano-powders by a citrate complex method and its photoluminescence property. *Journal of alloys and compounds* **2005**, *390*, 245-249, <https://doi.org/10.1016/j.jallcom.2004.07.064>.
5. Fu, H.; Lin, J.; Zhang, L.; Zhu, Y. Photocatalytic activities of a novel $ZnWO_4$ catalyst prepared by a hydrothermal process. *Applied Catalysis A: General* **2006**, *306*, 58-67, <https://doi.org/10.1016/j.apcata.2006.03.040>.
6. Sundaram, R.; Nagaraja, K.S. Electrical and humidity sensing properties of lead(II) tungstate-tungsten(VI) oxide and zinc(II) tungstate-tungsten(VI) oxide composites. *Materials Research Bulletin* **2004**, *39*, 581-590, <https://doi.org/10.1016/j.materresbull.2003.12.014>.
7. Li, H.; Wang, D.; Fan, H.; Wang, P.; Jiang, T.; Xie, T. Synthesis of highly efficient C-doped TiO_2 photocatalyst and its photo-generated charge-transfer properties. *Journal of Colloid and Interface Science* **2011**, *354*, 175-180, <https://doi.org/10.1016/j.jcis.2010.10.048>.

found to be greater than 5 the sample is considered to be in single magnetic domain. If the squareness is smaller than 5, the material synthesized has multiple fields [33,34]. The sample in our project has squareness less than 5.

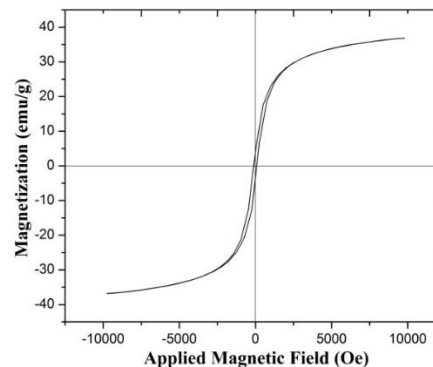


Figure 7. Magnetic hysteresis characterization of copper zinc cobalt ferrites systems (CZCFO NCs) nano composites.

acknowledged by (SAED) profile. The specific absorption rate is found to be inversely proportional to the concentration of the sample. The degradation efficiency of MB, under UV light is 72% with an increase in time duration.

8. Nolan, N.T.; Synnott, D.W.; Seery, M.K.; Hinder, S.J.; Van Wassenhoven, A.; Pillai, S.C. Effect of N-doping on the photocatalytic activity of sol-gel TiO_2 . *Journal of Hazardous Materials* **2012**, *211-212*, 88-94, <https://doi.org/10.1016/j.jhazmat.2011.08.074>.
9. Cheng, X.; Wang, P.; Liu, H. Visible-light-driven photoelectrocatalytic degradation of diclofenac by N, S-TiO₂/TiO₂ NTs photoelectrode: performance and mechanism study. *Journal of Environmental Chemical Engineering* **2015**, *3*, 1713-1719, <https://doi.org/10.1016/j.jece.2015.06.015>.
10. Kerkez-Kuyumcu, Ö.; Kibar, E.; Dayıoğlu, K.; Gedik, F.; Akın, A.N.; Özkara-Aydınoglu, Ş. A comparative study for removal of different dyes over M/TiO₂ (M=Cu, Ni, Co, Fe, Mn and Cr) photocatalysts under visible light irradiation. *Journal of Photochemistry and Photobiology A: Chemistry* **2015**, *311*, 176-185, <https://doi.org/10.1016/j.jphotochem.2015.05.037>.
11. Inturi, S.N.R.; Boningari, T.; Suidan, M.; Smirniotis, P.G. Visible-light-induced photodegradation of gas phase acetonitrile using aerosol-made transition metal (V, Cr, Fe, Co, Mn, Mo, Ni, Cu, Y, Ce, and Zr) doped TiO_2 . *Applied Catalysis B: Environmental* **2014**, *144*, 333-342, <https://doi.org/10.1016/j.apcatb.2013.07.032>.
12. Ramos, D.D.; Bezerra, P.C.S.; Quina, F.H.; Dantas, R.F.; Casagrande, G.A.; Oliveira, S.C.; Oliveira, M.R.S.; Oliveira, L.C.S.; Ferreira, V.S.; Oliveira, S.L., et al. Synthesis and characterization of TiO_2 and TiO_2/Ag for use in photodegradation of methylviologen, with kinetic study by laser flash photolysis. *Environmental Science and Pollution Research* **2015**, *22*, 774-783, <https://doi.org/10.1007/s11356-014-2678-1>.
13. Etacheri, V.; Di Valentin, C.; Schneider, J.; Bahnemann, D.; Pillai, S.C. Visible-light activation of TiO_2 photocatalysts: Advances in theory and experiments. *Journal of Photochemistry and Photobiology C: Photochemistry Reviews* **2015**, *25*, 1-29, <https://doi.org/10.1016/j.jphotochemrev.2015.08.003>.

14. Fernández-Rodríguez, C.; Doña-Rodríguez, J.M.; González-Díaz, O.; Seck, I.; Zerbani, D.; Portillo, D.; Perez-Peña, J. Synthesis of highly photoactive TiO₂ and Pt/TiO₂ nanocatalysts for substrate-specific photocatalytic applications. *Applied Catalysis B: Environmental* **2012**, *125*, 383-389, <https://doi.org/10.1016/j.apcatb.2012.04.042>.
15. Manikandan, A.; Arul Antony, D.S. Magnetically separable Mn_xZn_{1-x}Fe₂O₄; (0.0 ≤ x ≤ 0.5) nanostructures: Structural, morphological, opto-magnetic and photocatalytic properties. *Synthesis and Reactivity in Inorganic, Metal-Organic, and Nano-Metal Chemistry* **2015**, *46*, <https://doi.org/10.1080/15533174.2015.1004454>.
16. Manikandan, A.; Durka, M.; Seevakan, K.; Arul Antony, D.S. A Novel One-Pot Combustion Synthesis and Opto-magnetic Properties of Magnetically Separable Spinel Mn_xMg_{1-x}Fe₂O₄ (0.0 ≤ x ≤ 0.5) Nanophotocatalysts. *Journal of Superconductivity and Novel Magnetism* **2014**, *28*, 1405-1416, <https://doi.org/10.1007/s10948-014-2864-x>.
17. Manikandan, A.; Durka, M.; Antony, S.A. A Novel Synthesis, Structural, Morphological, and Opto-magnetic Characterizations of Magnetically Separable Spinel Co_xMn_{1-x}Fe₂O₄ (0 ≤ x ≤ 1) Nano-catalysts. *Journal of Superconductivity and Novel Magnetism* **2014**, *27*, 2841-2857, <https://doi.org/10.1007/s10948-014-2771-1>.
18. Snelling, E.C. *Soft Ferrites: Properties and Applications*. 1st ed., Newnes-Butterworth, 1969.
19. Wang, Y.M.; Cao, X.; Liu, G.H.; Hong, R.Y.; Chen, Y.M.; Chen, X.F.; Li, H.Z.; Xu, B.; Wei, D.G. Synthesis of Fe₃O₄ magnetic fluid used for magnetic resonance imaging and hyperthermia. *Journal of Magnetism and Magnetic Materials* **2011**, *323*, 2953-2959, <https://doi.org/10.1016/j.jmmm.2011.05.060>.
20. Zhang, L.; Jiao, W. The effect of microstructure on the gas properties of NiFe₂O₄ sensors: Nanotube and nanoparticle. *Sensors and Actuators B: Chemical* **2015**, *216*, 293-297, <https://doi.org/10.1016/j.snb.2015.04.049>.
21. Casbeer, E.; Sharma, V.K.; Li, X.-Z. Synthesis and photocatalytic activity of ferrites under visible light: A review. *Separation and Purification Technology* **2012**, *87*, 1-14, <https://doi.org/10.1016/j.seppur.2011.11.034>.
22. Xu, S.-H.; Feng, D.-L.; Li, D.-X.; Shanguan, W.-F. Preparation of Magnetic Photocatalyst TiO₂ Supported on NiFe₂O₄ and Effect of Magnetic Carrier on Photocatalytic Activity. *Chinese Journal of Chemistry* **2008**, *26*, 842-846, <https://doi.org/10.1002/cjoc.200890156>.
23. Ciocarlan, R.G.; Pui, A.; Gherca, D.; Virilan, C.; Dobromir, M.; Nica, V.; Craus, M.L.; Gostin, I.N.; Caltun, O.; Hempelman, R.; Cool, P. Quaternary M_{0.25}Cu_{0.25}Mg_{0.5}Fe₂O₄ (M=Ni, Zn, Co, Mn) ferrite oxides: Synthesis, characterization and magnetic properties. *Materials Research Bulletin* **2016**, *81*, 63-70, <https://doi.org/10.1016/j.materresbull.2016.05.001>.
24. He, H.Y.; Yan, Y.; Huang, J.F.; Lu, J. Rapid photodegradation of methyl blue on magnetic Zn_{1-x}Co_xFe₂O₄ nanoparticles synthesized by hydrothermal process. *Separation and Purification Technology* **2014**, *136*, 36-41, <https://doi.org/10.1016/j.seppur.2014.08.028>.
25. Makovec, D.; Drogenik, M. Non-stoichiometric zinc-ferrite spinel nanoparticles. *Journal of Nanoparticle Research* **2008**, *10*, 131-141, <https://doi.org/10.1007/s11051-008-9400-5>.
26. Sivakumar, M.; Takami, T.; Ikuta, H.; Towata, A.; Yasui, K.; Tuziuti, T.; Kozuka, T.; Bhattacharya, D.; Iida, Y. Fabrication of zinc ferrite nanocrystals by sonochemical emulsification and evaporation: observation of magnetization and its relaxation at low temperature. *J Phys Chem B* **2006**, *110*, 15234-15243, <http://dx.doi.org/10.1021/jp055024c>.
27. Rameshbabu, R.; Ramesh, R.; Kanagesan, S.; Karthigeyan, A.; Ponnusamy, S. One pot facile hydrothermal synthesis of superparamagnetic ZnFe₂O₄ nanoparticles and their properties. *Journal of Sol-Gel Science and Technology* **2014**, *71*, 147-151, <https://doi.org/10.1007/s10971-014-3347-z>.
28. Bhosale, R.R.; Kumar, A.; AlMomani, F.; Alxneit, I. Propylene oxide assisted sol-gel synthesis of zinc ferrite nanoparticles for solar fuel production. *Ceramics International* **2016**, *42*, 2431-2438, <https://doi.org/10.1016/j.ceramint.2015.10.043>.
29. Dom, R.; Subasri, R.; Hebalkar, N.Y.; Chary, A.S.; Borse, P.H. Synthesis of a hydrogen producing nanocrystalline ZnFe₂O₄ visible light photocatalyst using a rapid microwave irradiation method. *RSC Advances* **2012**, *2*, 12782-12791, <http://dx.doi.org/10.1039/c2ra21910g>.
30. Raeisi Shahraki, R.; Ebrahimi, M.; Seyyed Ebrahimi, S.A.; Masoudpanah, S.M. Structural characterization and magnetic properties of superparamagnetic zinc ferrite nanoparticles synthesized by the coprecipitation method. *Journal of Magnetism and Magnetic Materials* **2012**, *324*, 3762-3765, <https://doi.org/10.1016/j.jmmm.2012.06.020>.
31. Charles Prabakar, A.; Sathyaseelan, B.; Killivalavan, G.; Iruson, B.; Senthilnathan, K.; Manikandan, E.; Sivakumar, D. Photocatalytic dye degradation properties of Zinc Copper Ferrites nanoparticles. *Journal of Nanostructures* **2019**, *9*, 694-701.
32. Tahir Farid, H.M.; Ahmad, I.; Bhatti, K.A.; Ali, I.; Ramay, S.M.; Mahmood, A. The effect of praseodymium on Cobalt-Zinc spinel ferrites. *Ceramics International* **2017**, *43*, 7253-7260, <https://doi.org/10.1016/j.ceramint.2017.03.016>.
33. Akther Hossain, A.K.M.; Rahman, M.A.; Farhad, S.F.U.; Vilquin, B.; Tanaka, H. Effect of Li substitution on the magnetic properties of Li_xMg_{0.40}Ni_{0.60-2x}Fe_{2+x}O₄ ferrites. *Physica B: Condensed Matter* **2011**, *406*, 1506-1512, <https://doi.org/10.1016/j.physb.2011.01.058>.
34. Ali, R.; Mahmood, A.; Khan, M.A.; Chughtai, A.H.; Shahid, M.; Shakir, I.; Warsi, M.F. Impacts of Ni-Co substitution on the structural, magnetic and dielectric properties of magnesium nanoferrites fabricated by micro-emulsion method. *Journal of Alloys and Compounds* **2014**, *584*, 363-368, <https://doi.org/10.1016/j.jallcom.2013.08.114>.
35. Saffari, F.; Kameli, P.; Rahimi, M.; Ahmadvand, H.; Salamati, H. Effects of Co-substitution on the structural and magnetic properties of NiCo_xFe_{2-x}O₄ ferrite nanoparticles. *Ceramics International* **2015**, *41*, 7352-7358, <https://doi.org/10.1016/j.ceramint.2015.02.038>.
36. Ateia, E.E.; Soliman, F.S. Modification of Co/Cu nanoferrites properties via Gd³⁺/Er³⁺ doping. *Applied Physics A: Materials Science and Processing* **2017**, *123*, <https://doi.org/10.1007/s00339-017-0948-8>.

